

RESEARCH PAPER

Compact power divider based on half mode substrate integrated waveguide (HMSIW) with arbitrary power dividing ratio

ALI-REZA MOZNEBI AND KAMBIZ AFROOZ

Design and realisation of a compact power divider based on half mode substrate integrated waveguide (HMSIW) with an arbitrary power dividing ratio is presented. This design consists of a substrate integrated waveguide (SIW) transition, two bisected HMSIW transitions by a gap, an SIW-to-microstrip transition, and two microstrip feed lines. In addition, a resistor is attached between two HMSIW transitions. To adjust the power division ratio, four parameters are introduced. Furthermore, four graphs are plotted using a three-dimensional electromagnetic (3D EM) simulator to graphically determine the introduced parameters. In this study, three circuits with power division ratios of 1:1, 1:4, and 1:8 are simulated using the 3D EM simulator and fabricated on a Rogers RO4003C substrate. The results show a good agreement between the simulated and measured results. The measured results display these circuits (1:1, 1:4, and 1:8) have the bandwidths of 70, 36, and 40%, respectively. Moreover, the proposed structures (1:1, 1:4, and 1:8) are compact and their overall sizes are $1.13 \times 1.04\lambda_g^2$, $0.96 \times 0.91\lambda_g^2$, and $0.81 \times 0.78\lambda_g^2$, respectively. These structures have the advantages of the compactness in size, wide bandwidth, high power division ratio (from 1:1 to 1:16), and compatibility with planar circuits.

Keywords: Power divider, Arbitrary power division, Half mode substrate integrated waveguide (HMSIW), Compact size

Received 30 September 2015; Revised 21 March 2016; Accepted 30 March 2016; first published online 2 May 2016

I. INTRODUCTION

Power divider is one of the fundamental devices in microwave and millimeter-wave circuits such as mixers, power amplifiers, and phase-array antennas [1–3]. Microstrip transmission lines have been widely used in power dividers because of compatibility with planar circuits and simple manufacturing process. But in these structures, the electromagnetic leakage and coupling are serious problems at high frequencies that limit their applications.

Conventional waveguide power dividers have the advantages of high Q-factor and low loss capacity [4, 5]. But, these structures suffer from problems of high cost, bulky volume, and difficult integration with planar circuits [6]. Recently, substrate integrated waveguide (SIW) structure is introduced [7, 8]. The SIW is configured by metallic via holes, as shown in Fig. 1. This structure has the benefits of the low loss, low cost, high Q-factor, and easy integration with planar circuits [9]. The size of the SIW is relatively large. The half mode substrate integrated waveguide (HMSIW) can be considered by separating the SIW along the propagation direction, which is an equivalent magnetic

wall [10]. By this work, compared with the SIW, the size of the structure is reduced by nearly 50%.

Several power dividers based on SIW and HMSIW have been investigated [11–20]. In [14], a Y-junction four-way power divider was reported. This power divider had the large insertion loss. The reported circuit in [16] had the large insertion loss and large phase imbalance. Among these SIW/HMSIW power dividers, two T-junction SIW power dividers with arbitrary power division ratio were introduced in [19] and [20]. But these power dividers had the disadvantages of the large insertion loss and big size because the T-junction nature is comparatively large size.

In this paper, a compact power divider based on HMSIW with an arbitrary power dividing ratio is proposed. Three circuits with power division ratios of 1:1, 1:4, and 1:8 are presented. These structures consist of an SIW transition, two bisected HMSIW transitions by a gap, an SIW-to-microstrip transition in the input port at the left side, two microstrip feed lines in the output ports at the right side, and a resistor between the two HMSIW transitions. In the circuit of the equal power divider, this resistor is just added to achieve the isolation between the output ports. But their value and location, the angle of the gap with the propagation direction, and the length of the gap are the parameters of the power management in the two other circuits. Four graphs are plotted using a three-dimensional electromagnetic (3D EM) simulator to graphically determine the introduced parameters. Figure 2 shows the configuration of these circuits. Moreover, the used SIW-to-microstrip transition is introduced in [21].

Department of Electrical Engineering, Shahid Bahonar University of Kerman, Kerman, Iran. Phone: +98 34 31322516

Corresponding author:

K. Afrooz

Email: afrooz@uk.ac.ir

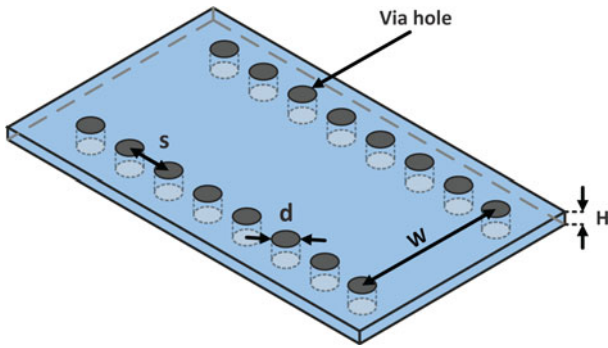


Fig. 1. Configuration of a SIW structure.

It features two vias, which have the same diameter as the SIW vias and are located symmetrically at both sides of the microstrip taper. These designs are simulated using the 3D EM simulator and fabricated on a Rogers RO4003C substrate. The results show a good agreement between the simulated and measured results. The measured results display these circuits (1:1, 1:4, and 1:8) have the bandwidths of 70, 36, and 40%, respectively.

II. DESIGN PROCEDURE

A) SIW and HMSIW design

As shown in Fig. 2(a), one SIW transition is used and two HMSIW transitions are separated with a gap between them. The TE_{10} is the dominant mode of the SIW structure. The

cutoff frequency is obtained by [3]:

$$f_{cmn} = \frac{c}{2\pi\sqrt{\mu_r\epsilon_r}} \sqrt{\left(\frac{m\pi}{W_{eff}}\right)^2 + \left(\frac{n\pi}{h}\right)^2}. \tag{1}$$

In this case, the cutoff frequency is the same as conventional rectangular waveguide. In (1), m and n are the mode indexes, c is the velocity of light in the free space, ϵ_r is the relative permittivity of the substrate, μ_r is the relative permeability of the substrate, h refers to the height, and W_{eff} refers to the equivalent width of the SIW, which is equal to [22]:

$$W_{eff} = W - 1.08 \cdot \frac{d^2}{s} + 0.1 \cdot \frac{d^2}{W}. \tag{2}$$

In (2), d refers to the diameter of the vias, s is their longitudinal spacing, and W displays the transverse spacing of the two vias that are located at both sides of the SIW. In this structure, the transverse magnetic (TM) modes cannot be guided due to the dielectric gaps created by the via separations [23]. For the better performance of the circuit, d and s are limited as follows [24]:

$$\frac{s}{d} \leq 2. \tag{3}$$

B) SIW-to-microstrip transition and microstrip feed lines design

In the input, a microstrip-to-SIW transition is used based on [21]. After designing the microstrip and SIW parameters, the

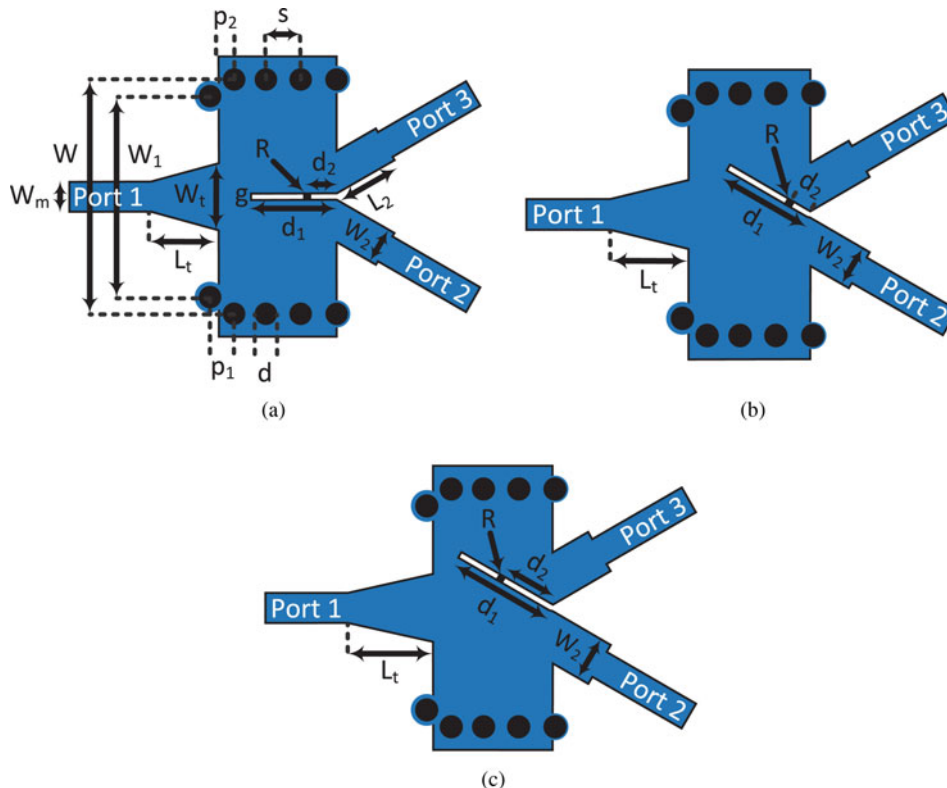


Fig. 2. Configuration of the proposed structures: (a) $\Delta_{out} = 0$ dB, (b) $\Delta_{out} = 6$ dB, and (c) $\Delta_{out} = 9$ dB.

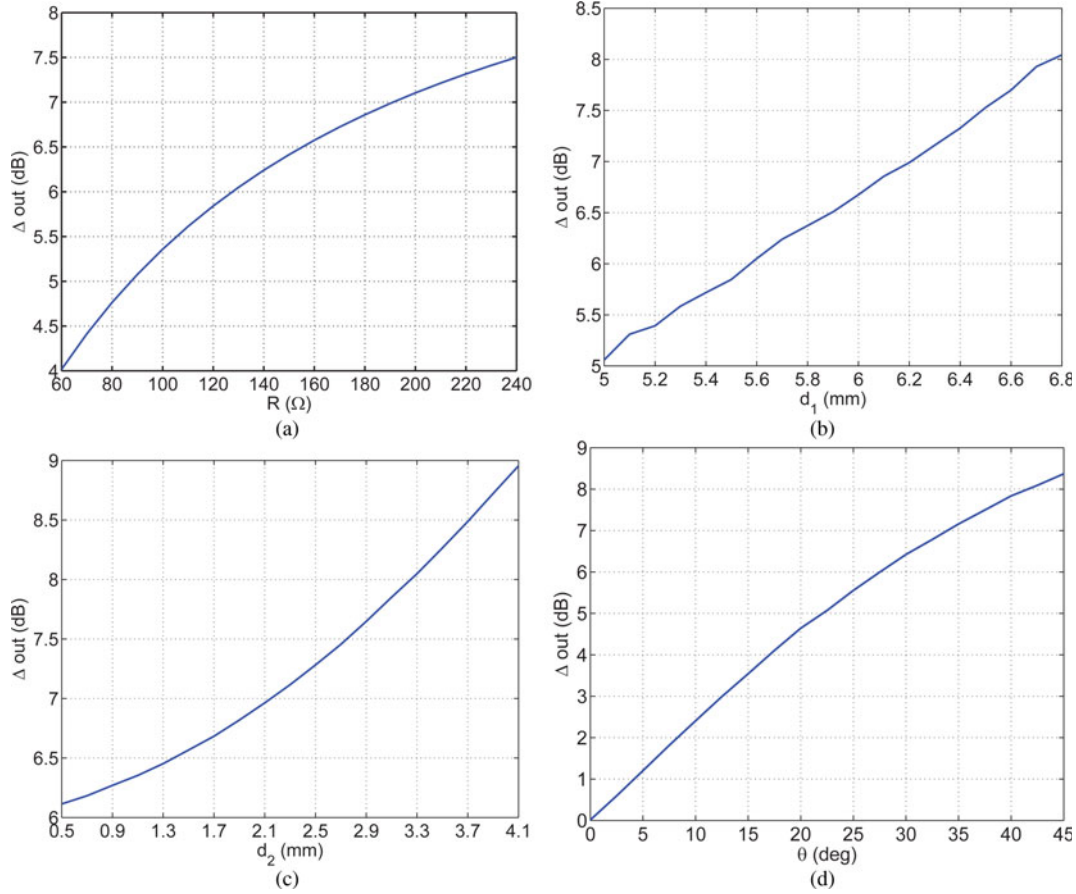


Fig. 3. Values of Δ_{out} versus different: (a) R when $\theta = 30^\circ$, $d_1 = 5.83$ mm, and $d_2 = 1.21$ mm, (b) d_1 when $R = 150 \Omega$, $\theta = 30^\circ$, and $d_2 = 1.21$ mm, (c) d_2 when $R = 150 \Omega$, $\theta = 30^\circ$, and $d_1 = 5.83$ mm, (d) θ when $R = 150 \Omega$, $d_1 = 5.83$ mm, and $d_2 = 1.21$ mm.

taper-via transition parameters can be calculated as [21]:

$$L_t = 0.2368\lambda_{gMS}, \tag{4}$$

$$W_t = W_m + 0.1547W, \tag{5}$$

$$p_1 = 0.6561s, \tag{6}$$

$$W_1 = 0.8556W. \tag{7}$$

λ_{gMS} is the guided wavelength of the microstrip line calculated at the center frequency

$$\lambda_{gMS} = \frac{\lambda_{go}}{\sqrt{\epsilon_{reff}}}. \tag{8}$$

In (8), ϵ_{reff} refers to the effective dielectric constant of the microstrip line and λ_{go} refers to the wavelength in free space. In the output, two microstrip feed lines are used. After designing the structure with 50Ω microstrip lines, by tuning the parameters of the microstrip feed lines (W_2 and L_2), excellent impedance matching can be achieved.

C) Determining R , θ , d_1 , and d_2

In this paper, the power management is realized by varying the value (R) and location of the resistor (d_2), the angle of the gap with the propagation direction (θ), and the length of the gap (d_1). To adjust the power division ratio, the value of θ is main parameter. If this parameter is equal to zero, then $\Delta_{out} = 0$ dB, and the parameters of R , d_1 , and d_2 have no effect on the power management. In the presented equal

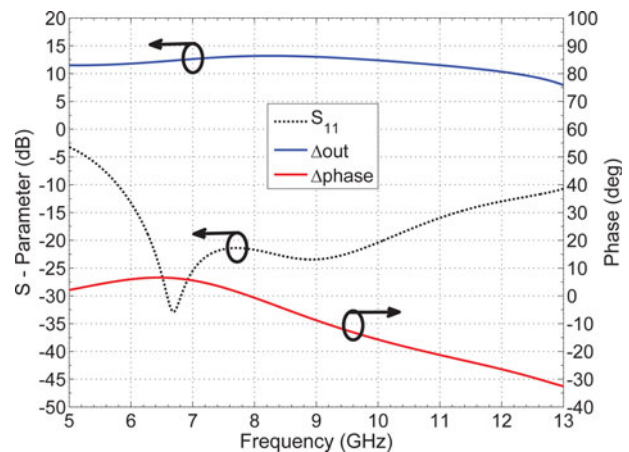
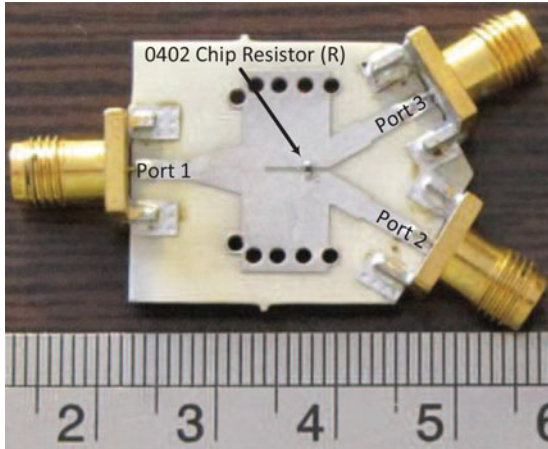


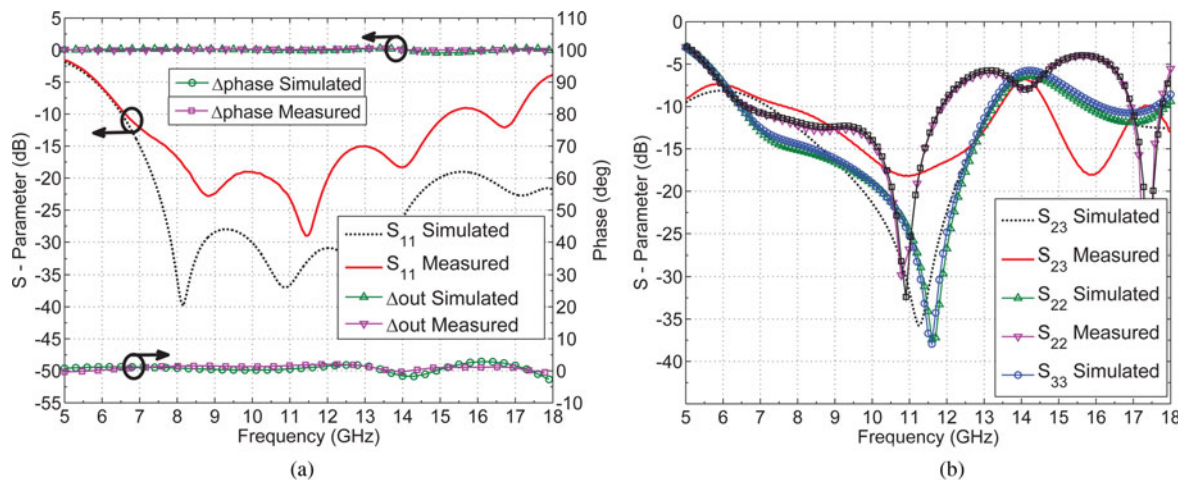
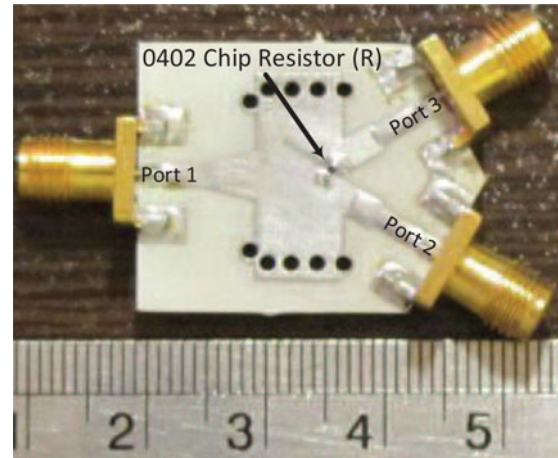
Fig. 4. Results of the compact HMSIW power divider with $\Delta_{out} = 12$ dB ($\theta = 45^\circ$, $R = 156 \Omega$, $d_1 = 6.75$ mm, and $d_2 = 3.57$ mm).

Table 1. Parameters of the proposed structures.

$\Delta_{out} = 0$ dB	W	14.65 (mm)	L_t	4.24 (mm)	p_2	1.11 (mm)
	W_1	12.56 (mm)	d	1.45 (mm)	s	2.18 (mm)
	W_2	2.28 (mm)	d_1	5.35 (mm)	g	0.4 (mm)
	W_t	4.19 (mm)	d_2	1.85 (mm)	R	47 (Ω)
	L_2	4.15 (mm)	p_1	1.5 (mm)	θ	0 ($^\circ$)
$\Delta_{out} = 6$ dB	W_2	2.54 (mm)	d_1	5.83 (mm)	R	150 (Ω)
	L_t	4.74 (mm)	d_2	1.21 (mm)	θ	30 ($^\circ$)
$\Delta_{out} = 9$ dB	W_2	2.79 (mm)	d_1	6.67 (mm)	R	150 (Ω)
	L_t	5.25 (mm)	d_2	3.23 (mm)	θ	30 ($^\circ$)

**Fig. 5.** Photograph of the compact HMSIW power divider with $\Delta_{out} = 0$ dB.

power divider, the used resistor is attached between two HMSIW transitions to improve the isolation and return loss of the output ports. The parameters of R , d_1 , and d_2 are arisen by increasing the value of θ . Figure 3 shows the values of Δ_{out} versus different R , θ , d_1 , and d_2 . This figure is obtained by changing the values of the introduced parameters. As shown in Fig. 3, the power difference between the output ports can be increased by increasing R , θ , d_1 , and d_2 . From Fig. 3(d), it can be concluded that the proposed structure can obtain the high power division ratio.

**Fig. 6.** Simulated and measured results of the compact HMSIW power divider with $\Delta_{out} = 0$ dB: (a) S_{11} , Δ_{out} , and Δ_{phase} , (b) isolation (S_{23}) and the return loss of the output ports (S_{22} and S_{33}).**Fig. 7.** Photograph of the compact HMSIW power divider with $\Delta_{out} = 6$ dB.

Furthermore, by increasing the values of R , d_1 , and d_2 , the value of Δ_{out} can vary in a wider range (from 1:1 to 1:16). In order to prove it, an unequal power divider with $\Delta_{out} = 12$ dB is designed. Figure 4 shows the simulated results of the unequal power divider with $\Delta_{out} = 12$ dB.

Moreover, Table 1 displays the parameters of the proposed structures shown in Fig. 2.

III. SIMULATED AND MEASURED RESULTS

Three compact HMSIW power dividers with power division ratios of 1:1, 1:4, and 1:8 have been designed and fabricated on a single layer Rogers RO4003C substrate with a thickness, relative permittivity, and loss tangent of 0.8128 mm, 3.55, and 0.0027, respectively.

A) Compact HMSIW power divider with $\Delta_{out} = 0$ dB

In the equal power divider, the measured results illustrate the return loss is >12.5 dB for the fractional bandwidth of 70%

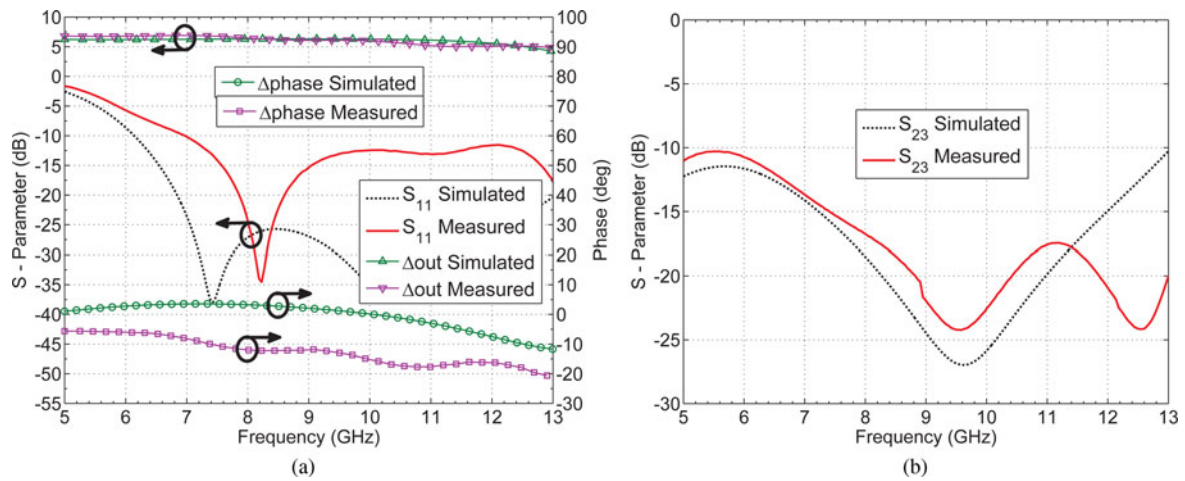


Fig. 8. Simulated and measured results of the compact HMSIW power divider with $\Delta out = 6$ dB: (a) S_{11} , Δout , and $\Delta phase$, (b) isolation (S_{23}).

(7.08–14.77 GHz). Moreover, Δout is < 0.3 dB and $\Delta phase$ is $< 2^\circ$. But the isolation between output ports and the return loss of the output ports are > 10 dB for the fractional bandwidth of 43% (7.67–11.87 GHz). The photograph of the fabricated equal power divider is shown in Fig. 5. Figures 6(a) and 6(b) depict the simulated and measured results of the proposed structure.

$< \Delta out \pm 10\%$, and $\Delta phase$ is $< 10^\circ$ when the return loss is better than 12.5 dB. The photograph of the fabricated unequal power divider with $\Delta out = 9$ dB is shown in Fig. 9. Figures 10(a) and 10(b) depict the simulated and measured results of the proposed structure. It should be noted here

B) Compact HMSIW power divider with $\Delta out = 6$ dB

In the unequal power divider with $\Delta out = 6$ dB, the measured fractional bandwidth is 36% (7.59–10.88 GHz), Δout is $< \Delta out \pm 12\%$, and $\Delta phase$ is $< 18^\circ$ when the return loss is better than 12.5 dB. The photograph of the fabricated unequal power divider with $\Delta out = 6$ dB is shown in Fig. 7. Figures 8(a) and 8(b) depict the simulated and measured results of the proposed structure.

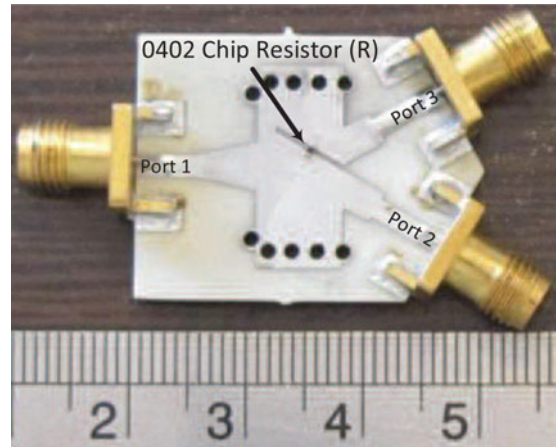


Fig. 9. Photograph of the compact HMSIW power divider with $\Delta out = 9$ dB.

C) Compact HMSIW power divider with $\Delta out = 9$ dB

In the unequal power divider with $\Delta out = 9$ dB, the measured fractional bandwidth is 40% (6.18–9.25 GHz), Δout is

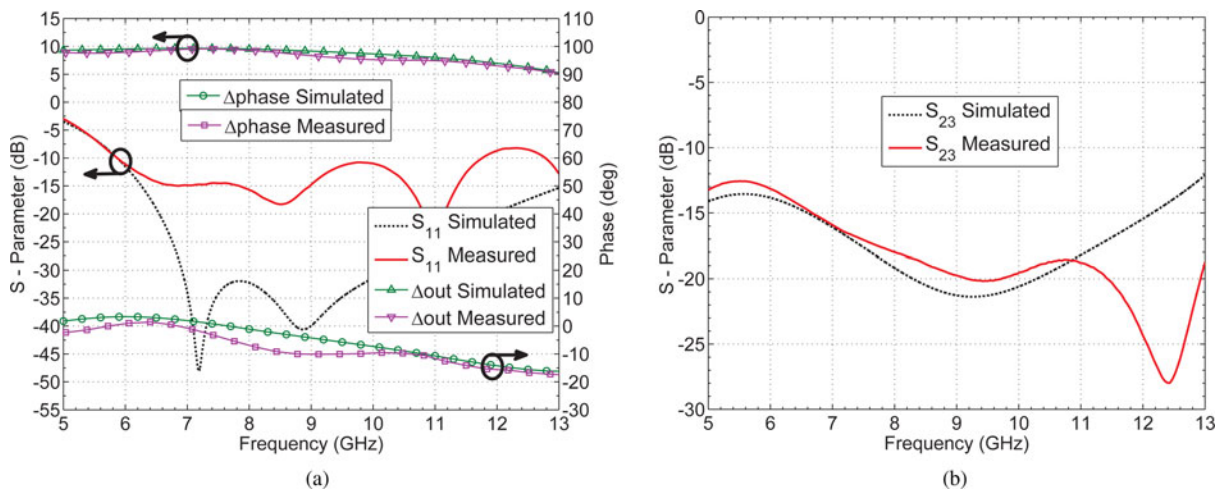


Fig. 10. Simulated and measured results of the compact HMSIW power divider with $\Delta out = 9$ dB: (a) S_{11} , Δout , and $\Delta phase$, (b) isolation (S_{23}).

Table 2. Comparison with other works.

$ dB(S_{21}) - dB(S_{31}) \leq \Delta out \pm 12\%$, $dB(S_{11}) \leq -12.5$ dB				
Reference	Δout (dB)	FBW (%)	Size (λ_g^2)	Structure
[17]	0	10.9	3.91×1.64	SIW Y-junction
[18]	0	23.5	1.5×0.95	Ring-shaped SIW
This Work	0	70	1.13×1.04	HMSIW
[19]	6	12.2	4.42×2.3	SIW T-junction
This Work	6	36	0.96×0.91	HMSIW
[25]	9	18	0.9×0.49	Microstrip
This Work	9	40	0.81×0.78	HMSIW

FBW: fractional bandwidth.

that the bandwidth is limited by both input matching and Δout variations.

The proposed structures (1:1, 1:4, and 1:8) are compact and have the overall sizes of $1.13 \times 1.04\lambda_g^2$, $0.96 \times 0.91\lambda_g^2$, and $0.81 \times 0.78\lambda_g^2$, respectively. This indicates that the proposed structures are a good candidate for compact HMSIW power divider with arbitrary power dividing ratio. Some slight differences between the measured and simulated results is mainly caused by the insertion loss of sub-miniature-A (SMA) connectors, fabrication errors, and the tolerance of the dielectric constant. In Table 2, a comparison between this work and other works is summarized.

IV. CONCLUSION

In this paper, a compact HMSIW power divider with an arbitrary power dividing ratio has been presented. Compared with the previously introduced structure, this unequal power divider can be widely used in millimeter-wave systems and microwave because of its simple and compactness in size.

REFERENCES

- [1] Wu, Y.; Liu, Y.; Xue, Q.; Li, S.; Yu, C.: Analytical design method of multiway dual-band planar power dividers with arbitrary power division. *IEEE Trans. Microw. Theory Tech.*, **58** (2010), 3832–3841.
- [2] Bahl, I.J.: Ultrabroadband and compact power dividers/combiners on gallium arsenide substrate. *IEEE Microw. Mag.*, **2** (2008), 96–104.
- [3] Pozar, D.M.: *Microwave Engineering*, 3rd ed., Wiley, USA, 2006.
- [4] Chen, X.P.; Wu, K.: Substrate integrated waveguide filter: basic design rules and fundamental structure features. *IEEE Microw. Mag.*, **15** (2014), 108–116.
- [5] Rui, M.; Mengjia, L.; Houjun, S.; Zhen, L.; Pei, Z.: Design and simulation of a W-band two-way power divider based on substrate integrated waveguide, in *Microw. Tech. & Computational Electromagnetics (ICMTCE)*, IEEE Int. Conf., 2013, 100–102.
- [6] Hao, Z.; Hong, W.; Li, H.; Zhang, H.; Wu, K.: Multiway broadband substrate integrated waveguide (SIW) power divider, in *IEEE Antennas and Propagation Society Int. Symp.*, vol. 1, 2005, 639–642.
- [7] Uchimura, H.; Takenoshita, T.; Fujii, M.: Development of a laminated waveguide. *IEEE Trans. Microw. Theory Tech.*, **46** (1998), 2438–2443.
- [8] Yan, L.; Hong, W.; Wu, K.; Cui, T.J.: Investigations on the propagation characteristics of the substrate integrated waveguide based on the method of lines. *IET Microw. Antennas Propag.*, **152** (2005), 35–42.
- [9] Bozzi, M.; Georgiadis, A.; Wu, K.: Review of substrate-integrated waveguide circuits and antennas. *IET Microw. Antennas Propag.*, **5** (2011), 909–920.
- [10] Hong, W. et al.: Half mode substrate integrated waveguide: A new guided wave structure for microwave and millimeter wave application, in *Proc. Joint 31st Int. Infrared Millimeter Wave Conf. 14th Int. Terahertz Electron. Conf.*, Shanghai, China, 2006, 18–22.
- [11] Smith, N.; Abhari, R.: Compact substrate integrated waveguide Wilkinson power dividers, in *IEEE Antennas and Propagation Society Int. Symp.*, 2009, 1–4.
- [12] Zhang, Z.Y.; Wu, K.: Broadband half-mode substrate integrated waveguide (HMSIW) Wilkinson power divider, in *IEEE Microw. Symp. Digest*, 2008, 879–882.
- [13] Jin, H.; Wen, G.: A novel four-way Ka-band spatial power combiner based on HMSIW. *IEEE Microw. Wireless Compon. Lett.*, **18** (2008), 515–517.
- [14] Zou, X.; Tong, C.M.; Yu, D.W.: Y-junction power divider based on substrate integrated waveguide. *Electron. Lett.*, **47** (2011), 1375–1376.
- [15] Hui, J.N.; Feng, W.J.; Che, W.Q.: Balun bandpass filter based on multilayer substrate integrated waveguide power divider. *Electron. Lett.*, **48** (2012), 571–573.
- [16] Rosenberg, U.; Salehi, M.; Bornemann, J.; Mehrshahi, E.: A novel frequency-selective power combiner/divider in single-layer substrate integrated waveguide technology. *IEEE Microw. Wireless Compon. Lett.*, **23** (2013), 406–408.
- [17] Kim, K.; Byun, J.; Lee, H.Y.: Substrate integrated waveguide Wilkinson power divider with improved isolation performance. *Progr. Electromagn. Res. Lett.*, **19** (2010), 41–48.
- [18] Djeraji, T.; Hammou, D.; Wu, K.; Tatu, S.O.: Ring-shaped substrate integrated waveguide Wilkinson power dividers/combiners. *IEEE Trans. Compon. Packag. Manuf. Technol.*, **4** (2014), 1461–1469.
- [19] Contreras, S.; Peden, A.: Graphical design method for unequal power dividers based on phase-balanced SIW tee-junctions. *Int. J. Microw. Wireless Technol.*, **5** (2013), 603–610.
- [20] Li, T.; Dou, W.: Broadband substrate-integrated waveguide T-junction with arbitrary power-dividing ratio. *Electron. Lett.*, **51** (2015), 259–260.
- [21] Kordiboroujeni, Z.; Bornemann, J.: New wideband transition from Microstrip line to substrate integrated waveguide. *IEEE Trans. Microw. Theory Tech.*, **62** (2014), 2983–2989.
- [22] Xu, F.; Wu, K.: Guided-wave and leakage characteristics of substrate integrated waveguide. *IEEE Trans. Microw. Theory Tech.*, **53** (2005), 66–73.
- [23] Rayas-Sánchez, J.E.; Gutierrez-Ayala, V.: A general EM-based design procedure for single-layer substrate integrated waveguide interconnects with microstrip transitions, in *IEEE Microw. Symp. Digest*, 2008, 983–986.
- [24] Wu, K.; Deslandes, D.; Cassivi, Y.: The substrate integrated circuits-a new concept for high-frequency electronics and optoelectronics, in *IEEE Telecommunications in Modern Satellite, Cable and Broadcasting Service*, 2003.
- [25] Li, B.; Wu, X.; Wu, W.: A 10:1 unequal Wilkinson power divider using coupled lines with two shorts. *IEEE Microw. Wireless Compon. Lett.*, **19** (2009), 789–791.



Ali-Reza Moznebi was born in Sirjan, Iran, in 1990. He received the B.S. degree in Electrical Engineering from O.T.F. University, Fars, Iran, in 2013, and the M.S. degree in Electrical Engineering from the Shahid Bahonar University of Kerman, Kerman, Iran, in 2016. He is currently working as a post-graduate scholar at the Department of

Electrical Engineering (Shahid Bahonar University of Kerman). His research interests include microwave/millimeter-wave power-dividing technology and microwave/millimeter-wave devices, circuits, and systems.



Kambiz Afrooz was born in Baft, Iran, in 1983. He received the B.Sc. degree from the Shahid Bahonar University of Kerman, Kerman, Iran, in 2005, the M.Sc. and Ph.D. degrees from the Amir-kabir University of Technology (Tehran Polytechnic), Tehran, Iran, in 2007 and 2012, respectively, all in Electrical Engineering. In May 2011, he joined

the CIMITEC group, University Autònoma de Barcelona

(UAB), Barcelona, Spain, as a Visiting Student. He is currently an Assistant professor with the Electrical Engineering Department, Shahid Bahonar University of Kerman, Kerman, Iran. His research interests include computer-aided design of active and passive microwave devices and circuits, computational electromagnetic, modeling and simulation of high-speed interconnects, metamaterial transmission lines, and substrate integrated waveguide structures. He is also the recipient of the Electrical Engineering Department Outstanding Student Award in 2007.